

Conductance fluctuations in quantum wires with spin-orbit and boundary-roughness scattering

T. Ando and H. Tamura

Institute for Solid State Physics, University of Tokyo, 7-22-1 Roppongi, Minato-ku, Tokyo 106, Japan

(Received 26 February 1992)

Conductance fluctuations in quantum wires with spin-orbit interaction and in those with boundary-roughness scattering are studied. In a length region much smaller than the localization length, a strong spin-orbit interaction reduces the fluctuation nearly by $\frac{1}{2}$ and boundary roughness causes fluctuations quite different from those for bulk scatterers. Once the localization effect becomes important, the fluctuations exhibit an almost universal length dependence if scaled by the localization length, irrespective of the kinds of scatterer and the symmetry of the system.

I. INTRODUCTION

Narrow wires can be fabricated by introducing a confining potential in a two-dimensional electron system at a modulation-doped GaAs/Al_xGa_{1-x}As heterostructure. In such quantum wires, the width is smaller than the mean free path and comparable to the Fermi wavelength, leading to the presence of well-defined one-dimensional (1D) subbands. In metallic wires, on the other hand, the electron motion is classical and also diffusive even in the transverse direction because the width is much larger than the mean free path and the Fermi wavelength. Thus, conductance fluctuations in quantum wires can be quite different from those in metallic wires which have been shown to be universal by various methods including perturbation calculations,¹⁻⁵ numerical calculations,⁶⁻¹⁵ and also analytic argument based on the random-matrix theory.¹⁶ In a previous paper, fluctuations in quantum wires were studied both in the presence and in the absence of a magnetic field.¹⁷ The purpose of this paper is to study effects of spin-orbit interaction and boundary-roughness scattering.

There are three different universality classes for the symmetry of systems: orthogonal, unitary, and symplectic.¹⁸ The orthogonal case corresponds to systems in the presence of time-reversal symmetry, where the Hamiltonian is represented by a real symmetric matrix and the corresponding wave function can be chosen as real. When a magnetic field is applied, the time-reversal symmetry is broken, and consequently wave functions become complex because the Hamiltonian becomes a complex Hermitian matrix. We have another symmetry called symplectic in the presence of spin-orbit interactions and the time-reversal symmetry. Perturbation calculations in metallic wires have shown that the fluctuation is reduced by $1/\sqrt{2}$ in the presence of a magnetic field and by $\frac{1}{2}$ in the presence of strong spin-orbit interaction.

Recent experiments have demonstrated that in long quantum wires scattering from boundary roughness gives rise to a large positive magnetoresistance.¹⁹ This positive magnetoresistance is similar to that observed in metallic thin films for which classical explanation is possible. The

classical theory²⁰ assumes that each electron is reflected specularly with the probability p and otherwise scattered into a random direction. In the absence of a magnetic field, the roughness itself cannot produce a nonzero resistivity because straight trajectories parallel to film surfaces have an infinite mean free path and dominate the current. In the presence of a magnetic field, the resistivity becomes nonzero because all electrons follow a curved trajectory and are scattered at collision with the boundaries.

A quantum-mechanical calculation of boundary-roughness scattering gives results analogous to those of the classical theory.²¹ In the absence of a magnetic field it causes a peculiar current distribution among 1D subbands such that most of the current is carried by low-lying subbands. This singular behavior nearly disappears and the current is almost equally shared by different 1D subbands in magnetic fields, leading to the positive magnetoresistance. Conductance fluctuations in the case of boundary-roughness scattering is expected to be quite different from those for bulk scatterers.

In this paper we study conductance fluctuations in quantum wires with strong spin-orbit interaction and boundary roughness within a lattice model. In Sec. II numerical results showing effects of spin-orbit interaction are presented after a brief description of the model and method. Effects of boundary-roughness scattering are discussed in Sec. III. A summary and conclusion are given in Sec. IV.

II. SPIN-ORBIT INTERACTION

A. Model and method

In contrast to a continuum model used in Ref. 17 we use a square-lattice model because it is quite convenient and handy in treating various effects such as spin-orbit interaction and boundary roughness. In particular, effects of spin-orbit interaction can easily be introduced by the model same as that adopted in the study of symmetry effects on localization,²² which simulates actual two-dimensional systems in n -channel inversion layers on surfaces of III-V semiconductors or at GaAs/Al_xGa_{1-x}As heterostructures. It is described by the

Hamiltonian:

$$\mathcal{H} = \sum_i \varepsilon_i c_{i\sigma}^\dagger c_{i\sigma} - \sum_{i,j} \sum_{\sigma,\sigma'} V(i,\sigma;j,\sigma') c_{i\sigma}^\dagger c_{j\sigma'}, \quad (2.1)$$

where $V(i,\sigma;j,\sigma') = V_x$ or V_y depending on the direction of the nearest-neighbor site in the x and y direction. We have, in matrix form,

$$V_x = \begin{bmatrix} V_1 & V_2 \\ -V_2 & V_1 \end{bmatrix}, \quad V_y = \begin{bmatrix} V_1 & -iV_2 \\ -iV_2 & V_1 \end{bmatrix}, \quad (2.2)$$

with V_1 and V_2 being spin-diagonal and off-diagonal elements, respectively, and

$$|\uparrow\rangle = \begin{bmatrix} 1 \\ 0 \end{bmatrix}, \quad |\downarrow\rangle = \begin{bmatrix} 0 \\ 1 \end{bmatrix}. \quad (2.3)$$

Effects of scatterings from bulk impurities are introduced through randomness of site energy ε_i distributed uniformly with width U ($-U/2 \leq \varepsilon_i + 4V_1 \leq U/2$). This lattice model corresponds to the wire containing high

concentration of scatterers with δ -function potentials, if we choose the parameters as follows:

$$n_i V_0^2 = a^2 \langle (\varepsilon_i + 4V_1)^2 \rangle = \frac{a^2 U^2}{12}, \quad (2.4)$$

where n_i is the concentration of scatterers in a unit area, V_0 is the strength, and a is the lattice constant. Although dominant scatterers in GaAs/Al_xGa_{1-x}As systems are believed to have long-range potential,^{23,24} which may cause a considerable reduction in effects of scattering in narrow wires;²⁵ the present short-range model is expected to be sufficient for the study of fluctuations.

In the following, we measure almost all the quantities in units of corresponding quantities in 2D, i.e., energy is measured in units of the Fermi energy E_F and length in units of the Fermi wavelength λ_F . In a 2D system without randomness ($\varepsilon_i = -4V_1$), the energy of an electron with wave vector $\mathbf{k} = (k_x, k_y)$ is given by an eigenvalue of the following 2×2 matrix:

$$\mathcal{H}(k) = \begin{bmatrix} 4V_1 - 2V_1(\cos k_x a + \cos k_y a) & -2V_2(i \sin k_x a + \sin k_y a) \\ -2V_2(-i \sin k_x a + \sin k_y a) & 4V_1 - 2V_1(\cos k_x a + \cos k_y a) \end{bmatrix}. \quad (2.5)$$

For small $k_x a$ and $k_y a$, this becomes

$$\mathcal{H}(k) = \begin{bmatrix} \hbar^2 k^2 / 2m & -2\hbar^2 k_s (ik_x + k_y) / 2m \\ -2\hbar^2 k_s (-ik_x + k_y) / 2m & \hbar^2 k^2 / 2m \end{bmatrix}, \quad (2.6)$$

with m being the effective mass and

$$\frac{V_1}{E_F} = \frac{\hbar^2}{2ma^2 E_F} = \left[\frac{1}{2\pi} \right]^2 \left[\frac{\lambda_F}{a} \right]^2, \quad \frac{V_2}{E_F} = \frac{1}{2\pi} \frac{\lambda_F}{a} \frac{k_s}{k_F}. \quad (2.7)$$

The energy takes a minimum along the circle defined by $k = k_s$ instead of $k = 0$. We choose k_s/k_F as the parameter characterizing the strength of spin-orbit interaction. The presence of such a k -linear term was first pointed out by Ohkawa and Uemura²⁶ in n -channel inversion layers on narrow-band-gap Hg_xCd_{1-x}Te. It is quite difficult, however, to obtain a reliable estimate of the absolute magnitude of the k -linear term.²⁷

The strength of bulk impurity scattering is characterized by the mean free path Λ . The randomness parameter is easily shown to be related to Λ through

$$\frac{U}{E_F} = \left[\frac{6\lambda_F^3}{\pi^3 a^2 \Lambda} \right]^{1/2}. \quad (2.8)$$

The calculation of the conductance proceeds in the way analogous to that described already²⁸ in the absence of spin-orbit interaction based on the multichannel version²⁹⁻³² of Landauer's conductance formula.³³

B. Results

In the numerical calculation we choose $\Lambda/\lambda_F = 50$ which is close to that in Ref. 17 and $\lambda_F/a = 8$. The typi-

cal number of samples is 10^4 . It has been checked that the results obtained in the present lattice model are same as those of Ref. 17 in the absence of spin-orbit interaction.

Figure 1 shows an example of calculated conductance as a function of length measured in units of Λ for $2W/\lambda_F = 5.25$ corresponding to the channel number 5. Two different averages, arithmetic and geometric, are shown together with the localization length α^{-1} obtained by fitting a straight line to the $\langle \ln G \rangle$ versus L curve, i.e., $\alpha = -\partial \langle \ln G \rangle / \partial L$. (Note that the localization length is twice as large as that defined in Ref. 17.) The initial decrease of the conductance in the near-ballistic regime ($L/\Lambda \lesssim 1$) does not depend on the strength of spin-orbit interaction, corresponding to the fact that the mean free path itself is not affected by the spin-orbit interaction. With further increase of the length, the conductance in the presence of spin-orbit interaction decreases much more slowly than in its absence, which leads to the increase of the localization length by a factor of about 3.

In the limit of large channel numbers N_c the localization length has been shown to be given by $\alpha^{-1} \propto N_c \beta$ where β is the so-called level-repulsion exponent ($\beta = 1$ for orthogonal, 2 for unitary, and 4 for symplectic universality classes) in the random-matrix theory.^{34,35} For systems with more general values of N_c , analytic considerations based on a Fokker-Planck equation for the distribution function of the conductance gave $\alpha^{-1} \propto (\beta N_c + 2 - \beta)$.³⁶⁻³⁸ The present numerical result is

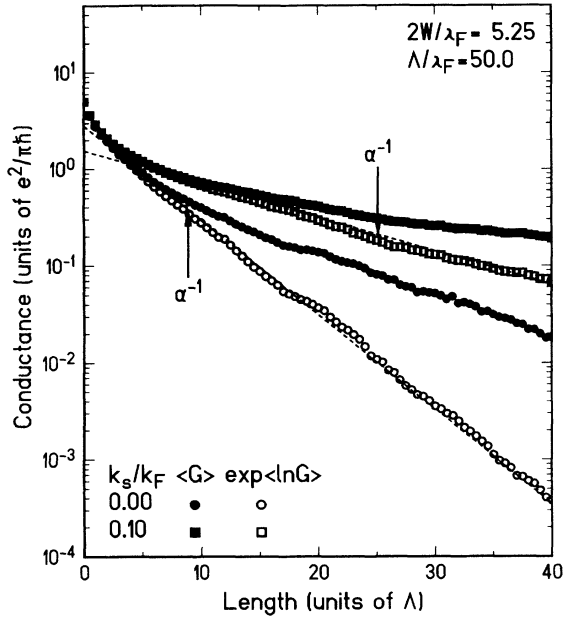


FIG. 1. Calculated conductance vs length in the presence (squares, $k_s/k_F=0.1$) and absence (circles) of spin-orbit interaction for wires with channel number 5. Two different averages, arithmetic (filled symbols) and geometric (open symbols), are shown. The vertical arrows denote the localization length α^{-1} . The dotted lines represent the straight lines corresponding to the localization length.

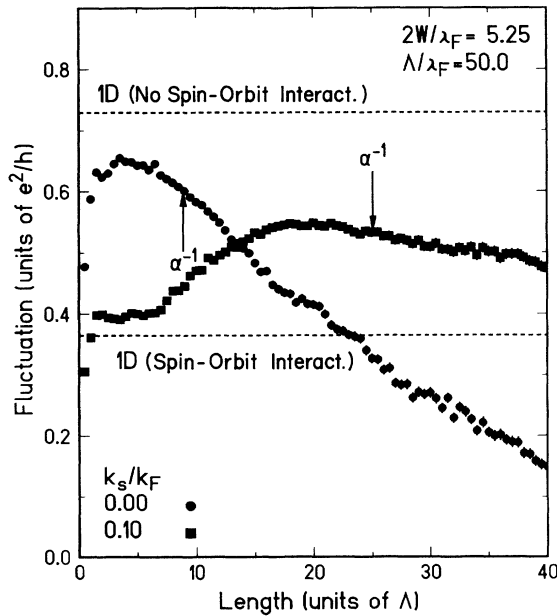


FIG. 2. Calculated conductance fluctuation vs length in the presence (squares, $k_s/k_F=0.1$) and absence (circles) of spin-orbit interaction for wires with channel number 5. The vertical arrows denote the localization length α^{-1} . The horizontal dotted lines represent the fluctuations calculated perturbationally for metallic 1D wires.

in good agreement with this analytic expression which shows that the localization length for $\beta=4$ is three times as large as that for $\beta=1$ in the case of $N_c=5$.

The corresponding result for the fluctuation is given in Fig. 2. In the absence of spin-orbit interaction the fluctuation increases first, takes a maximum, and starts to decrease gradually with the wire length.¹⁷ In the presence of spin-orbit interaction, the fluctuation is reduced by a factor close to $\frac{1}{2}$ for the length region much smaller than the localization length and larger than the mean free path (called universal region hereafter), but with further in-

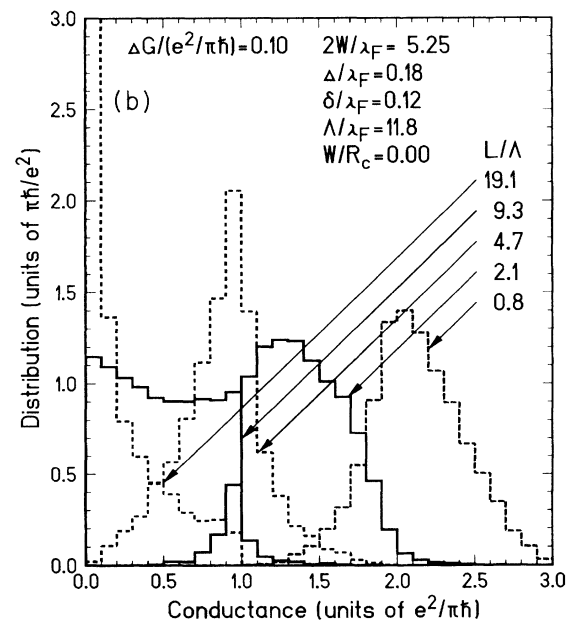
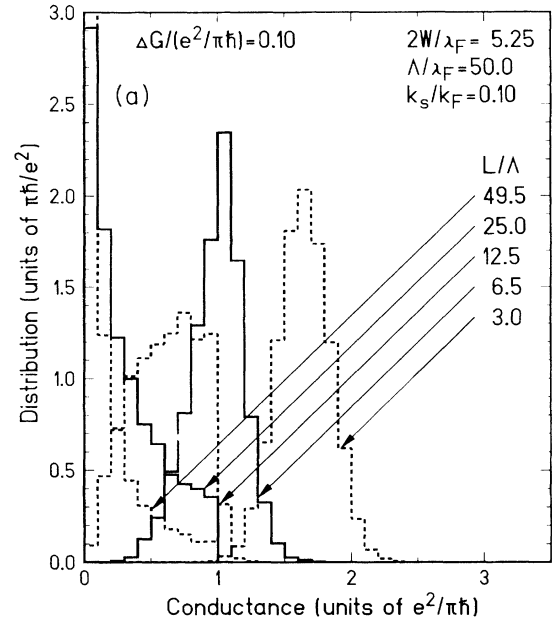


FIG. 3. Calculated histograms of the conductance in (a) the presence and (b) absence of spin-orbit interaction. The length of the wire L is chosen in such a way that $\alpha L \sim 2, 1, \frac{1}{2}, \frac{1}{4},$ and $\frac{1}{8}$ from the top.

crease of the length it gradually becomes larger and takes a maximum around the localization length. This feature is similar to that in weak magnetic fields.¹⁷

This length dependence may be more clearly understood if we look at the distribution function of the conductance. Figure 3 shows calculated distribution function corresponding to length $\alpha L \sim \frac{1}{8}, \frac{1}{4}, \frac{1}{2}, 1$, and 2. In the universal region the conductance nearly obeys a normal Gaussian distribution around the mean value. The width of the distribution is narrower in the presence of spin-orbit interaction than its absence. The distribution function undergoes a qualitative change when its left tail reaches the origin $G=0$. Because of the difference in the amount of the fluctuation, this change takes place at different lengths, $\alpha L \lesssim \frac{1}{4}$ in the presence of spin-orbit interaction and $\alpha L \lesssim \frac{1}{2}$ in its absence. For longer wires ($\alpha L \gtrsim 1$), the distribution function is nearly independent of the symmetry and close to that in a 1D wire.

In 1D wires an exact expression was derived by Abrikosov³⁹ for the distribution function of the conductance. Figure 4 shows the average conductance and fluctuation as a function of length and Fig. 5 gives the distribution function in a 1D wire. There is no length region where the conductance obeys a normal Gaussian distribution and the distribution function clearly changes its feature around a crossover length $L_c \lesssim \alpha^{-1}/2$ where its left tail reaches the origin. The fluctuation takes a maximum at a length slightly larger than L_c .

For wires much longer than the localization length ($\alpha L \gg 1$), the conductance and its fluctuation are essentially the same if the length is scaled by the localization length and thus independent of the channel number and symmetry. This can easily be understood because the conductance in the strong localization regime consists of sharp peaks at energies of localized states which are dis-

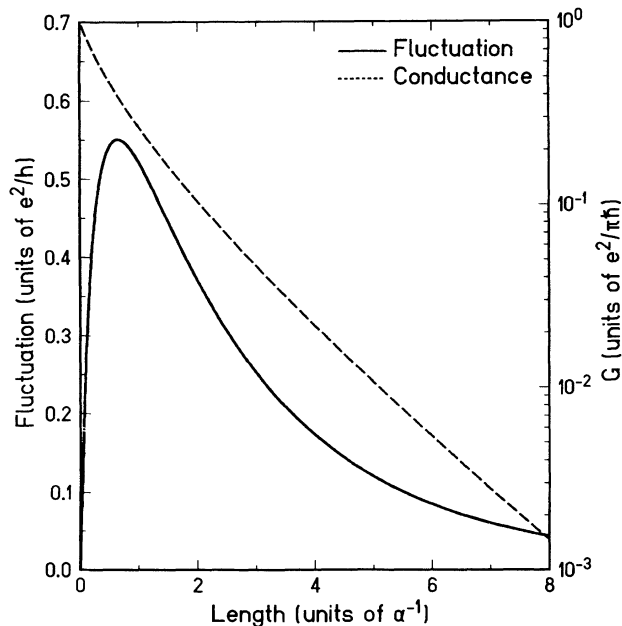


FIG. 4. Exact conductance (solid line) and fluctuation (dashed line) vs length in 1D wire.

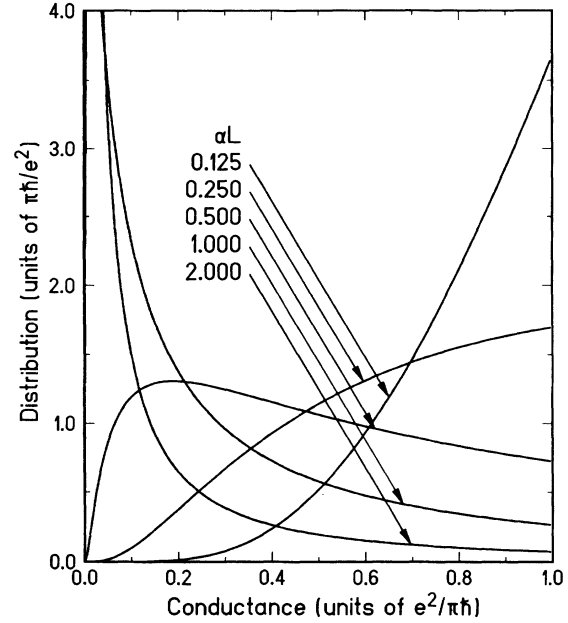


FIG. 5. Exact distribution function of the conductance in one-dimensional wire for several values of αL .

tributed almost randomly, have broadening determined by the localization length, and interact with each other only if their energies are very close.^{40,9} The present result suggests that this universality already prevails when $\alpha L \sim 1$.

Figure 6 shows calculated fluctuations for different values of k_s/k_F . The fluctuation takes a small maximum

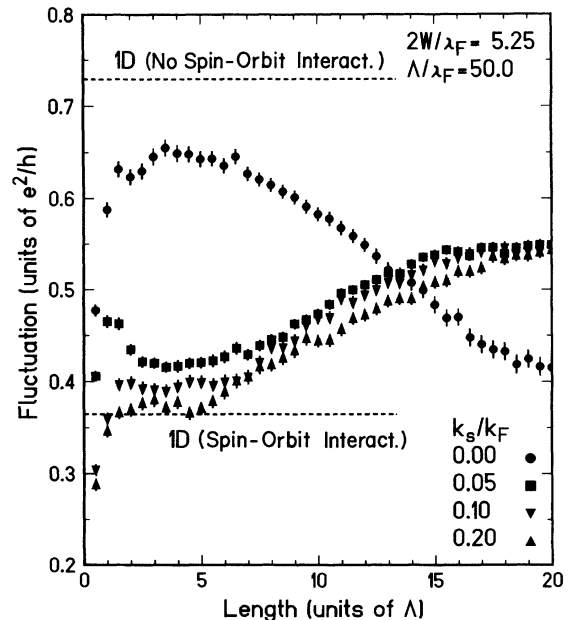


FIG. 6. Calculated conductance fluctuation vs length for several values of the spin-orbit parameter k_s/k_F . The horizontal dotted lines represent the fluctuations calculated perturbatively for metallic 1D wires.

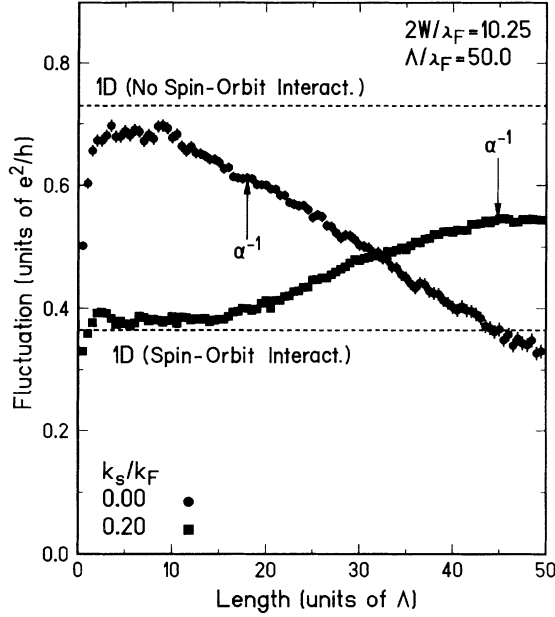


FIG. 7. Calculated conductance fluctuation vs length in the presence (squares) and absence (circles) of spin-orbit interaction for wires with channel number 10. The vertical arrows denote the localization length α^{-1} . The horizontal dotted lines represent the fluctuations calculated perturbationally for metallic 1D wires.

in the near-ballistic regime ($1 \lesssim \alpha L \lesssim 2$) particularly for weak spin-orbit interaction. This arises because electrons pass through the system before being affected by spin-flip scattering for such short wires. In other length region, the fluctuation does not depend on k_s/k_F appreciably as long as $k_s/k_F \neq 0$. This demonstrates that the symmetry is a key factor of determining fluctuations and localization.

Figure 7 gives calculated fluctuations for a wider wire with $2W/\lambda_F = 10.25$ corresponding to channel number 10. All the features are the same as those with $2W/\lambda_F = 5.25$ except that the universal region in the absence of spin-orbit interaction has become much clearer and the reduction due to the spin-orbit interaction has become further close to $\frac{1}{2}$.

III. BOUNDARY ROUGHNESS SCATTERING

The model of boundary roughness is chosen as exactly the same as that described in Ref. 21. The wire is separated into narrow sections whose length takes nd_0 ($n = 1, 2, \dots, n_d$) with probability n_d^{-1} . Within each section, the left and right boundaries are shifted by $\pm n\Delta_0$ ($n = 1, 2, \dots, n_\Delta$) with probability q/n_Δ and left unshifted with probability $1 - 2q$. This gives the following correlation function of roughness $\Delta_+(x)$ of the left boundary and $\Delta_-(x)$ of the right boundary:

$$\langle \Delta_\pm(x) \Delta_\mp(x') \rangle = \sqrt{\pi} \delta \Delta^2 g(x - x'), \quad (3.1)$$

with correlation length $\delta = (2n_d + 1)d_0/3\sqrt{\pi}$ and average displacement $\Delta^2 = q(n_\Delta + 1)(2n_\Delta + 1)\Delta_0^2/3$. The correla-

tion function $g(x)$ is normalized to unity and $g(0) = 1/\sqrt{\pi}\delta$.

Figure 8 shows calculated conductance for wires with boundary roughness as a function of the length normalized by the arithmetic average of the mean free path of each subband in the absence ($W/R_c = 0$) and presence ($W/R_c = 0.5$) of a magnetic field, where R_c is the classical cyclotron radius. In the Boltzmann transport theory, the conductivity is proportional to the arithmetic average and takes a minimum around a magnetic field corresponding to $W/R_c \sim 0.5$.²¹ The reduction in the mean free path from $\Lambda/\lambda_F \sim 11.8$ for $W/R_c = 0$ to $\Lambda/\lambda_F \sim 4.6$ for $W/R_c = 0.5$ shows that the resistivity is enhanced from its zero-field value by more than double in the Boltzmann transport theory.

The conductance for $W/R_c = 0$ does not agree with that for $W/R_c = 0.5$ in the near-ballistic regime ($L/\Lambda \lesssim 1$) even if scaled by the mean free path except at $L = 0$. This is to be expected because of the singularly strong dependence of the mean free path on 1D subbands. In the limit of short-range boundary roughness ($\delta/\lambda_F \ll 1$) the Boltzmann transport theory predicts that $\tau_n^{-1} \propto n^2$ for $W/R_c = 0$ where τ_n is the relaxation time of subband n . Because of an extra n dependence due to the velocity v_n the mean free path $\Lambda_n = \tau_n v_n$ exhibits even stronger dependence than n^{-2} . In fact, the actual calculation reveals that in the case of $2W/\lambda_F = 5.25$ the mean free path of the lowest subband is about two orders of

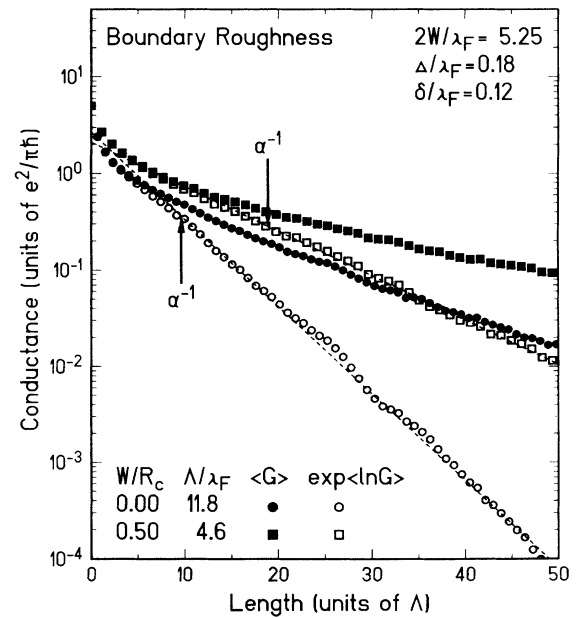


FIG. 8. Calculated conductance vs length in the presence (squares) and absence (circles) of a magnetic field for wires with channel number 5 having strong boundary roughness scattering (the correlation length $\delta/\lambda_F \sim 0.12$ and the mean deviation $\Delta/\lambda_F \sim 0.18$). Two different averages, arithmetic (filled symbols) and geometric (open symbols), are shown. The vertical arrows denote the localization length α^{-1} . The dotted lines represent the straight lines corresponding to the localization length.

magnitude larger than that of the highest subband. The decrease in the near-ballistic regime is likely to be determined by the harmonic average of Λ_n which is much smaller than Λ .

Figure 9 shows the corresponding fluctuation as a function of length. The fluctuation takes a sharp maximum in the near-ballistic regime ($L/\Lambda \lesssim 1$) and starts to decrease around the localization length in both absence and presence of a magnetic field. There is no universal region where the fluctuation remains independent of L presumably because the wire is still too narrow.

Figures 10 and 11 give the results for a wider wire with channel number 10 ($2W/\lambda_F = 10.25$). The magnetic-field reduction in the mean free path is much larger than that for $2W/\lambda_F = 5.25$. The universal region appears in the region $\Lambda \ll L < \alpha^{-1}$, where the fluctuation in the absence of a magnetic field is clearly smaller than that of 1D metallic wires but that in its presence is close to that of 1D metallic wires. The singular enhancement of the fluctuation in the near-ballistic regime is more profound for wider wires than narrower ones.

In short wires, mixing among different 1D subbands due to scattering is not appreciable and each channel may be regarded as almost independent. The transmission probability of the low-lying subbands has a sharper distribution with peak close to unity because of the large mean free path, while that of the higher subbands has a broader distribution with peak at much smaller than unity. This is presumably a main origin of the singular enhancement of the fluctuation in the near-ballistic regime. The enhancement may be related to the suggestion by Higurashi, Iwabuchi, and Nagaoka,⁴¹ who claimed that

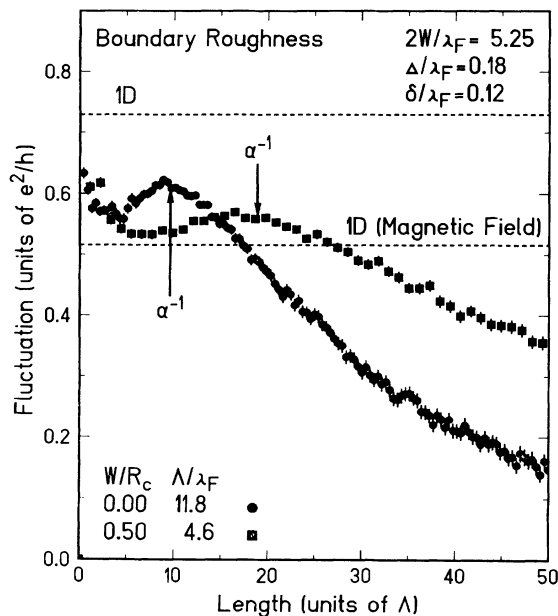


FIG. 9. Calculated conductance fluctuation vs length in the presence (squares) and absence (circles) of a magnetic field for wires with channel number 5 having strong boundary-roughness scattering. The vertical arrows denote the localization length α^{-1} . The horizontal dotted lines represent the fluctuations calculated perturbationally for metallic 1D wires.

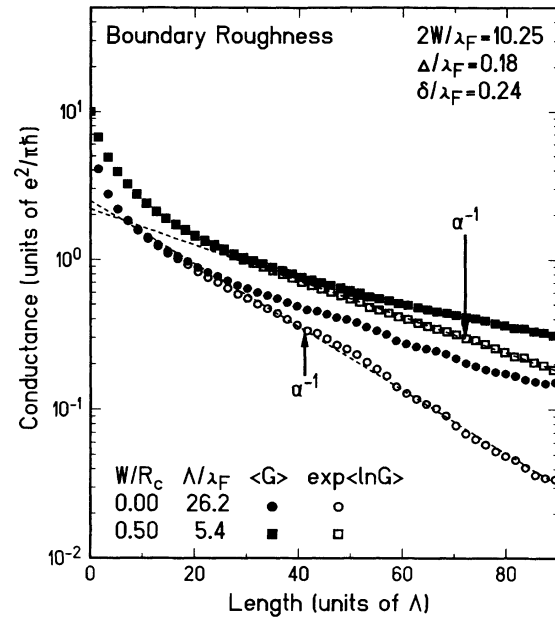


FIG. 10. Calculated conductance vs length in the presence (squares) and absence (circles) of a magnetic field for wires with channel number 10 having strong-boundary roughness scattering (the correlation length $\delta/\lambda_F \sim 0.24$ and the mean deviation $\Delta/\lambda_F \sim 0.18$). The dotted lines represent the straight lines corresponding to the localization length.

the fluctuation can be enhanced considerably in the near-ballistic regime even for bulk impurity scattering within a lattice model containing a peculiar anisotropy. In our model, which simulates actual quantum wires much better, however, such enhancement has not been obtained for bulk scatterers.¹⁷

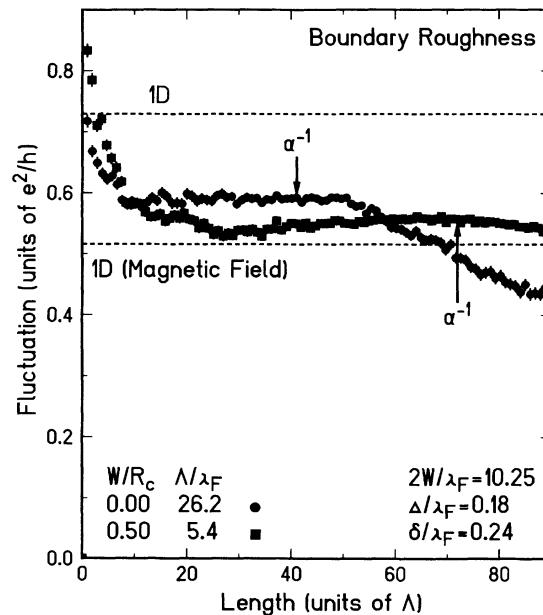


FIG. 11. Calculated conductance fluctuation vs length in the presence (squares) and absence (circles) of a magnetic field for wires with channel number 10 having strong boundary-roughness scattering.

IV. SUMMARY AND CONCLUSION

The conductance of quantum wires has been calculated within a lattice model in the presence of strong spin-orbit interaction and boundary-roughness scattering. The results are summarized as follows.

(i) The spin-orbit interaction reduces the fluctuation to nearly half of that in its absence in the universal region much larger than the mean free path and smaller than the localization length. This agrees with the conclusion obtained in perturbation calculations for 1D metallic wires. When the length becomes larger, the fluctuation increases, takes a maximum around the localization length, and then decreases with increasing length. This feature is quite similar to (but much more pronounced than) that in the presence of a weak magnetic field. This is closely related to the fact that the distribution function of the conductance becomes essentially that of a 1D wire when the length is comparable to or larger than the localization length.

(ii) Owing to the peculiar nature of boundary-roughness scattering, the conductance fluctuation exhibits behavior different from that for bulk impurities when the length is smaller than the localization length, i.e., a singular enhancement of the fluctuation in the near-ballistic regime and the reduction in the universal region from that of 1D metallic diffusive wires. When the localization effect becomes important, the fluctuation becomes the same as that for bulk impurity scattering if the length is scaled by the localization length.

ACKNOWLEDGMENTS

This work is supported in part by the Industry-University Joint Research Program "Mesoscopic Electronics" and by the Grants-in-Aid for Scientific Research on Priority Area, "Electron Wave Interference Effects in Mesoscopic Structures" and "Computational Physics as a New Frontier in Condensed Matter Research," from the Ministry of Education, Science and Culture, Japan.

-
- ¹B. L. Altshuler, Pis'ma Zh. Eksp. Theor. Fiz. **41**, 530 (1985) [JETP Lett. **41**, 648 (1985)].
- ²P. A. Lee and A. D. Stone, Phys. Rev. Lett. **55**, 1622 (1985).
- ³B. L. Altshuler and D. E. Khmel'nitskii, Pis'ma Zh. Eksp. Theor. Fiz. **42**, 291 (1985) [JETP Lett. **42**, 359 (1986)].
- ⁴P. A. Lee, A. D. Stone, and H. Fukuyama, Phys. Rev. B **35**, 1039 (1987).
- ⁵C. L. Kane, R. A. Serota, and P. A. Lee, Phys. Rev. B **37**, 6701 (1988).
- ⁶A. D. Stone, Phys. Rev. Lett. **54**, 2692 (1985).
- ⁷N. Giordano, Phys. Rev. B **36**, 4190 (1987).
- ⁸X. C. Xie and S. Das Sarma, Phys. Rev. B **38**, 3529 (1988).
- ⁹K. Tankei, A. Sawada, and Y. Nagaoka, J. Phys. Soc. Jpn. **58**, 368 (1989).
- ¹⁰B. Kramer, J. Masek, V. Spicka, and B. Velicky, Surf. Sci. **229**, 316 (1990).
- ¹¹S. Datta, M. Cahay, and M. McLennan, Phys. Rev. B **36**, 5655 (1987).
- ¹²M. Cahay, M. McLennan, and S. Datta, Phys. Rev. B **37**, 10 125 (1988).
- ¹³M. Cahay, S. Bandyopadhyay, M. A. Osman, and H. L. Grubin, Surf. Sci. **228**, 301 (1990).
- ¹⁴S. Bandyopadhyay, M. Cahay, D. Berman, and B. Nayfeh, Superlatt. and Microstruct. **10**, 327 (1991).
- ¹⁵R. Harris and A. Houari, Phys. Rev. B **41**, 5487 (1990).
- ¹⁶Y. Imry, Europhys. Lett. **1**, 249 (1986).
- ¹⁷H. Tamura and T. Ando, Phys. Rev. B **44**, 1792 (1991).
- ¹⁸F. J. Dyson, J. Math. Phys. **3**, 140 (1962); **3**, 157 (1962); **3**, 166 (1962); **3**, 1191 (1962); **3**, 1199 (1962).
- ¹⁹T. J. Thornton, M. L. Roukes, A. Scherer, and B. P. Van de Gaag, Phys. Rev. Lett. **63**, 2128 (1989).
- ²⁰K. Fuchs, Proc. Cambridge Phil. Soc. **34**, 100 (1938).
- ²¹H. Akera and T. Ando, Phys. Rev. B **43**, 11 676 (1991).
- ²²T. Ando, Phys. Rev. B **40**, 5325 (1989).
- ²³T. Ando, J. Phys. Soc. Jpn. **51**, 3900 (1982).
- ²⁴T. Ando and Y. Murayama, J. Phys. Soc. Jpn. **54**, 1519 (1985).
- ²⁵H. Sakaki, Jpn. J. Appl. Phys. **19** L735 (1980).
- ²⁶F. J. Ohkawa and Y. Uemura, J. Phys. Soc. Jpn. **37**, 1325 (1974).
- ²⁷See, for example, T. Ando, A. B. Fowler, and F. Stern, Rev. Mod. Phys. **54**, 437 (1982).
- ²⁸T. Ando, Phys. Rev. B **44**, 8017 (1991).
- ²⁹D. S. Fisher and P. A. Lee, Phys. Rev. B **23**, 6851 (1981).
- ³⁰M. Büttiker, Phys. Rev. Lett. **57**, 1761 (1986); Phys. Rev. B **38**, 9375 (1988).
- ³¹A. D. Stone and A. Szafer, IBM J. Res. Dev. **32**, 384 (1988).
- ³²H. U. Baranger and A. D. Stone, Phys. Rev. B **40**, 8169 (1989).
- ³³R. Landauer, IBM J. Res. Dev. **1**, 223 (1957); Philos. Mag. **21**, 863 (1970).
- ³⁴K. B. Efetov and A. I. Larkin, Zh. Eksp. Theor. Fiz. **85**, 764 (1983) [Sov. Phys. JETP **58**, 444 (1983)].
- ³⁵J.-L. Pichard, M. Sanquer, K. Slevin, and P. Debray, Phys. Rev. Lett. **65**, 1812 (1990).
- ³⁶O. N. Dorokhov, Zh. Eksp. Theor. Fiz. **85**, 1040 (1983) [Sov. Phys. JETP **58**, 606 (1983)].
- ³⁷J.-L. Pichard, in *Quantum Coherence in Mesoscopic Systems*, edited by B. Kramer (Plenum, New York, 1991), p. 369.
- ³⁸H. Tamura and T. Ando, in *Proceedings of Taniguchi Symposium on Physics of Mesoscopic Systems, Shima, 1991*, edited by H. Fukuyama and T. Ando (Springer, Heidelberg, in press).
- ³⁹A. A. Abrikosov, Phys. Scr. **T27**, 148 (1989).
- ⁴⁰P. W. Anderson, D. J. Thouless, E. Abrahams, and D. S. Fisher, Phys. Rev. B **22**, 3519 (1980).
- ⁴¹H. Higurashi, S. Iwabuchi, and Y. Nagaoka, Surf. Sci. **263**, 382 (1992).